Dynamic Analysis of Beams on Two-Parameter Viscoelastic Pasternak Foundation Subjected to the Moving Load and Considering Effects of Beam Roughness

T. Tran-Quoc, H. Nguyen-Trong and T. Khong-Trong

Abstract In this paper, improved moving element method (IMEM) is intended to analyze the dynamic response of the beam resting on the two-parameter viscoelastic Pasternak foundation subjected to the moving load and considering effects of beam roughness. Beams are modeled by moving elements, while the load is fixed. The differential equation of motion of the structural system is established based on the principle of virtual public balance and solved by means of numerical integration based on the Newmark algorithm. The characteristic parameters of the foundation and the loads are investigated in order to analyze the dynamic response of the beam such as the second parameter of foundation, the roughness of beam, the velocity and acceleration of moving load.

Keywords Moving element method · Beam · Foundation · Dynamic
Roughness amplitude · Roughness wavelength · Moving load

1 Introduction

Beam and plate structures are applied widely in the construction field nowadays. The topic of the structural beam on the soil–foundation interaction is much attracted and interested by many foreign and Vietnamese scientists. Majority of constructions for building and traffic infrastructures are built up on the soil–foundation interaction, so the scope of this application is wide. The moving load on structure is also

T. Tran-Quoc · H. Nguyen-Trong (✉) · T. Khong-Trong (✉)
Faculty of Civil Engineering, HUTECH University, Ho Chi Minh, Vietnam
e-mail: tronghieu221287@gmail.com

T. Khong-Trong
e-mail: kt.toan@hutech.edu.vn

T. Tran-Quoc
e-mail: quachtinhxd3012@gmail.com

represented by many researchers by different variety of types such as moving force, moving mass, various moving forces, moving vehicles. The foundation alone when analyzing the behavior of the structure which is described very complicated the same as the one-parameter foundation model such as Winkler [1] or multiparameter foundation models of Filonenko-Borodich [2], Hentényi [3], Pasternak [4], Reissner [5]. The typical characteristics of these models are that the elastic layer (the first parameter) that is illustrated based on the elastic Winkler foundation, with the stiffness of elastic foundation layer which is represented by the non-mass elastic springs; in respect to the multiparameter models, the second parameter is presented by the stress layer elements, beams or bending plates or shear layers without the mass of connection with the surface of springs on Winkler foundation model in order to describe the continuous interaction of foundation. Therefore, a more realistic model is needed for soil foundation under the loads of moving mass. Because of its wide and realistic application, this issue is concerned deeply by many researchers such as Chang-Yong and Yang [6], and they have analyzed the infinite Euler–Bernoulli beam resting on Pasternak foundation subjected to moving load which has constant velocity obtained by Fourier transformation technique to solve the problem. Kumari et al. [7] have investigated an infinite Euler–Bernoulli beam on Pasternak foundation; the beam is put placed on a concentrated mass which is equal to the constant motion, and the velocity is equal to beam's parameters.

Recently, many models of structures resting on viscoelastic and Pasternak foundation have been developed. Luong-Van et al. [8] and Phung-Van et al. [9] analyzed dynamics response of composite plates resting on viscoelastic foundation. Phung-Van et al. [10] analyzed dynamics response of Mindlin plates on viscoelastic foundation subjected to a moving sprung vehicle. Nguyen-Thoi et al. [11] analyzed the dynamics response of composite plates on the Pasternak foundation subjected to moving mass.

Lou and Au [12] have studied the response of Euler–Bernoulli beam under moving mass vehicles by employing a finite element method (FEM). FEM has been used widely to solve many complicated problems, but encountered issues when the mass moves to the margin of the elements and also from one element to another, while vector of moving mass must be updated at every time step. So as to make good those shortcomings, Koh et al. [13] have proposed to put a moving coordinate to solve the proposed moving mass of railway track. This method is called moving element method (MEM). In this method, the railway is considered as an infinite Euler–Bernoulli resting on beam on Winkler foundation and the train is simplified by a "mass-spring-dashpot" system. Tran et al. [14] have employed MEM to study the dynamic response of express railway under inconstant speed of moving mass. Ang et al. [15] have studied a calculation to employ MEM to examine the dynamic response of the rail on viscoelastic foundation with moving mass. Ang and Dai [16] analyzed the reaction of the high-speed railway on foundation which has inconstant stiffness, and the author employed the moving element method to have analytical solutions for the response of the train. Ang et al. [17] have used MEM to research the dynamic response of the railway system. The railway model as a mass spring system which includes train body, cross section and wheels. Recently, Tran et al. [18] also

utilized the moving element method to analyze the dynamics of the express railway. In which the railway track is modeled as based on Euler–Bernoulli beam on the elastic two-parameter, the impacts of reducing velocity process and the roughness levels of railway track are also investigated. MEM has a lot of advantages such as the load would never approach the margin because the limited elements system always moves, and the moving load would not have to move from this element to another, so it avoids updating the mass vector. This method enables the limited elements with different lengths, and each interaction distance can be divided more effective. However, the weak point of MEM is that must be re-updated the stiffness matrix and dashpot matrix at every time step. It resulted in increasing the volume of calculation, prolonging the time of analysis, and wasting the resources.

Therefore, this paper introduces one new method, that is, improved moving element (IMEM) to analyze the dynamic response of the beam resting on viscoelastic two-parameter Pasternak foundation which is under moving mass and with the consideration of beam surface. The mass matrices, the stiffness matrices, and dashpot matrices of the moving elements are also represented in details later on. All results obtained will be the helpful documents for studying and designing the structural beams placed on moving loads in reality.

2   Theoretical Basis

Investigating an infinite Euler–Bernoulli beam with elastic module E, moment of inertia I, and mass per unit length of the rail beam $\bar{m}$, beam is on a viscoelastic foundation comprising of dashpots $\bar{c}$, vertical springs $\bar{k}_w$, cross section k_s. Figure 1 shows the beam model, foundation, and load that are applied in this research.

Fig. 1 Train–track model
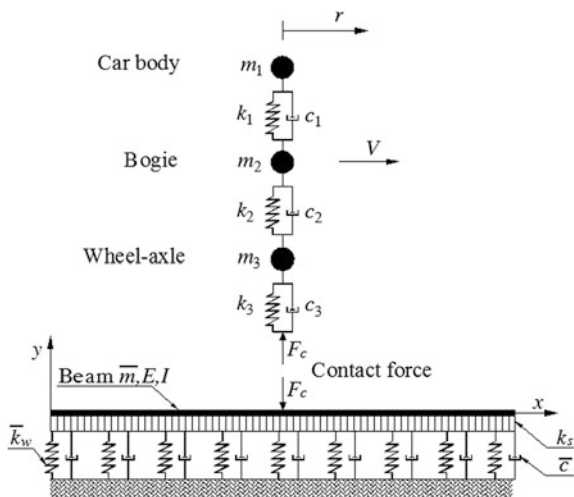
According to the coordinates in Fig. 1, the general equation of the car model Do and Luong [19] can be expressed mathematically as follows

$$m_1 \ddot{u}_1 + c_1(\dot{u}_1 - \dot{u}_2) + k_1(u_1 - u_2) = -m_1 g \tag{1}$$

$$m_2 \ddot{u}_2 + c_2(\dot{u}_2 - \dot{u}_3) - c_1(\dot{u}_1 - \dot{u}_2) + k_2(u_2 - u_3) - k_1(u_1 - u_2) = -m_2 g \tag{2}$$

$$m_3 \ddot{u}_3 - k_2(u_2 - u_3) - c_2(\dot{u}_2 - \dot{u}_3) = -m_3 g + F_c \tag{3}$$

in which:

m_1, m_2, m_3; c_1, c_2, c_3; k_1, k_2, k_3	in turn are mass, dashpots of the car, vertical springs, and wheels;
u_1, $\dot{u}_1$, $\ddot{u}_1$; u_2, $\dot{u}_2$, $\ddot{u}_2$; u_3, $\dot{u}_3$, $\ddot{u}_3$	in turn vertical displacements, velocity, car body acceleration, and wheel and axle;
g	gravitational acceleration;
F_c	the contact force between wheels and beam, produced by the non-flat of the beam or the roughness of the beam.

The contact force F_c (with the roughness at the contact point between the moving load and the beam) is defined according to Koh et al. [13] as follows:

$$F_c = c_3(\dot{u}_d - \dot{u}_3) + k_3(u_d - u_3) + F_t \tag{4}$$

where:

|	
$F_t = c_3 \dot{y}_t + k_3 y_t$	the track force, produced by the roughness of the beam;
u_d	denotes the vertical displacement at the contact point of the beam;
u_3	denotes the vertical displacement of the wheel and axle;
y_t	denotes the magnitude of the track irregularity at the contact point, and according to Koh et al. [13], the track irregularity profile can be written in terms of a sinusoidal function as follows:

$$y_t = a_t \sin \frac{2\pi S}{\lambda_t} \tag{5}$$

where:

a_t, λ_t	denotes the amplitude and wavelength of the track irregularity, respectively;
S	denotes the displacement of the object.

In the moving element method, Koh et al. [13] use x-y coordinates where x-axis is the beam course. The moving r-y coordinates whose origin is attached to the contact force as in Fig. 2. Therefore, this coordinates move along with the velocity V as a moving load.

Fig. 2 Coordinates of MEM
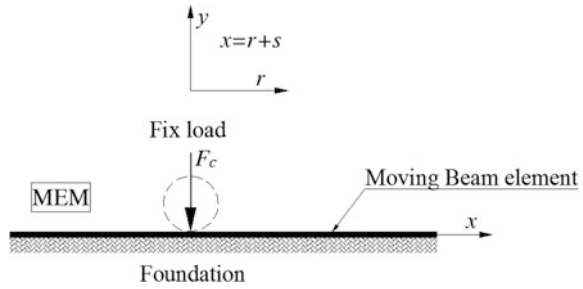
The relationship between two axes of coordinates is demonstrated as follows:

$$\begin{cases} x = r + s \\ y = y \end{cases} \tag{6}$$

where: x = fixed axis; r = movable axis; s = displacement; $V(a,t)$ = velocity function; t = moving time; a = acceleration.

The connection between the derivative operators of the coordinates when the load moves with various velocities is as follows:

$$\frac{\partial^4 w(x,t)}{\partial x^4} = \frac{\partial^4 w^*(r,t)}{\partial r^4} \tag{7}$$

$$\frac{\partial^2 w(x,t)}{\partial x^2} = \frac{\partial^2 w^*(r,t)}{\partial r^2} \tag{8}$$

$$\frac{\partial w(x,t)}{\partial t} = \frac{\partial w^*(r,t)}{\partial t}\frac{\partial t}{\partial t} + \frac{\partial w^*(r,t)}{\partial r}\frac{\partial r}{\partial t} = \frac{\partial w^*(r,t)}{\partial t} - V\frac{\partial w^*(r,t)}{\partial r} \tag{9}$$

$$\frac{\partial^2 w(x,t)}{\partial t^2} = \frac{\partial^2 w^*(r,t)}{\partial t^2} - a\frac{\partial w^*(r,t)}{\partial r}\frac{\partial r}{\partial t} + V^2\frac{\partial^2 w^*(r,t)}{\partial r^2} - 2V\frac{\partial^2 w^*(r,t)}{\partial r.\partial t} \tag{10}$$

where $w(x, t)$ = transverse deflection of the beam in the x-y axial coordinates; $w^*(r, t)$ = deflection of the beam in r-y coordinates.

By applying principle of virtual work and using displacement functions N, we can write $\mathbf{M^e}$, $\mathbf{C^e}$, $\mathbf{K^e}$ as generalized mass, damping and stiffness matrices of the beam as follows:

$$\mathbf{M}^e = \bar{m}\int_0^{l^e} \mathbf{N}^T\mathbf{N}\,dr \tag{11}$$

$$\boldsymbol{C}^e = \bar{c}\int_0^{l^e} \mathbf{N}^T\mathbf{N}\,dr - \mathbf{F}_1^e \tag{12}$$

$$\mathbf{K}^e = EI \int_0^{l^e} (\mathbf{N}_{,rr})^T \mathbf{N}_{,rr} dr + \bar{k}_w \int_0^{l^e} \mathbf{N}^T \mathbf{N} dr - k_s \int_0^{l^e} \mathbf{N}^T \mathbf{N}_{,rr} dr - \mathbf{F}_2^e \qquad (13)$$

$$\mathbf{F}_1^e = 2\bar{m}V \int_0^{l^e} \mathbf{N}^T \mathbf{N}_{,r} dr \qquad (14)$$

$$\mathbf{F}_2^e = [\bar{m}a + \bar{c}V] \int_0^{l^e} \mathbf{N}^T \mathbf{N}_{,r} dr - \bar{m}V^2 \int_0^{l^e} \mathbf{N}^T \mathbf{N}_{,rr} dr \qquad (15)$$

$$\mathbf{P} = \int_0^{l^e} F_c \mathbf{N}^T dr \qquad (16)$$

with $(.)_r$ and $(.)_{rr}$ in turn are first derivative and second derivative of r.

To elements of the beam, the Hermitian interpolation N is written as follows:

$$\mathbf{N}_1^e = \frac{1}{(l^e)^3} \left[2r^3 - 3r^2 l^e + (l^e)^3 \right] \qquad (17)$$

$$\mathbf{N}_2^e = \frac{1}{(l^e)^3} \left[r^3 l^e - 2r^2 (l^e)^2 + r(l^e)^3 \right] \qquad (18)$$

$$\mathbf{N}_3^e = \frac{1}{(l^e)^3} \left[-2r^3 + 3r^2 l^e \right] \qquad (19)$$

$$\mathbf{N}_4^e = \frac{1}{(l^e)^3} \left[r^3 l^e - r^2 (l^e)^2 \right] \qquad (20)$$

Based on finite element method and using numeral degree of freedom technique, respectively, to matrices of the general coordinates' elements, the moving equation of the whole beam model on the foundation is written as follows:

$$\mathbf{M}\ddot{\mathbf{z}} + (\mathbf{C} - \mathbf{F}_1)\dot{\mathbf{z}} + (\mathbf{K} - \mathbf{F}_2)\mathbf{z} = \mathbf{P} \qquad (21)$$

where:

M, C, K, P,   respectively, are global mass, damping and stiffness matrices, and the global load vector;

$\mathbf{F_1}$, $\mathbf{F_2}$ denote those elements which depend on time; $\mathbf{F_1}$ and $\mathbf{F_2}$ are not forces but have the force unit so they can be considered to be pseudo-force

Equation (21) is the main differential equation of the traditional MEM; in Eq. (21), we can see the left side is comprised of elements which change over time, and those elements are the pseudo-force $\mathbf{F_1}$ and $\mathbf{F_2}$ matrices. Therefore, when solving the problem we need to update the global mass, damping and stiffness matrices and this prolongs the processing time.

To fix this limitation of the traditional MEM, we like to move the pseudo-forces from the left side of Eq. (21) to the right side. This idea is called IMEM. After the moving, Eq. (21) is written as follows:

$$\mathbf{M\ddot{z}} + \mathbf{C\dot{z}} + \mathbf{Kz} = \mathbf{P} + \mathbf{F_1\dot{z}} + \mathbf{F_2z} \tag{22}$$

Solving the differential motion, Eq. (22) is put to act upon the help of computer which is based on Newmark algorithm. This algorithm is a calculation program written by MATLAB language, and the reliability as well as the calculation method of the program are put to compare to the results of other authors which are available in the reference.

3   Equation, Figure, and Table

3.1   Verifying the Calculation Program

In this part, the article examines some numerical examples to verify the correctness and the reliability of the MATLAB program. The results are compared to those of other authors.

Here is the verification of the high-speed train moving on beam with hanging mass which is used by Koh et al. [13] Fig. 1. The parameters of the train, the beam, and the foundation are demonstrated in Tables 1 and 2.
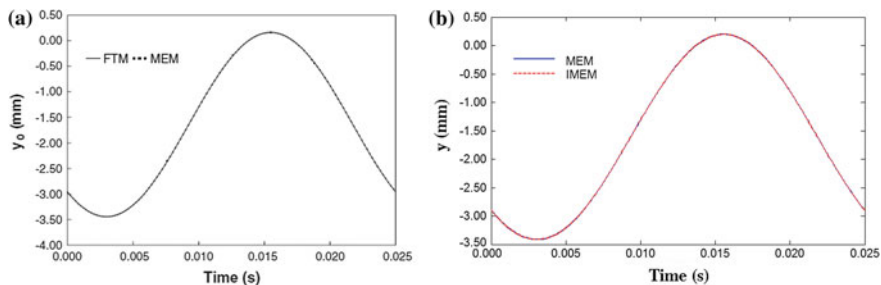
In the first example, the displacement of the beam while the train is moving on the beam with constant velocity, without consideration of the second foundation parameter affection (velocity $V = 20$ m/s, roughness amplitude margin $a_t = 0.5$ mm and roughness wavelength $\lambda_t = 0.5$ m) (Fig. 3).

Table 1 Parameters for vehicle

| Car Body		Bogie		Wheel and axle	
m_1	3500 kg	m_2	250 kg	m_3	350 kg
k_1	1.41×10^5 N/m	k_2	1.26×10^6 N/m	k_3	8×10^9 N/m
c_1	8.87×10^3 Ns/m	c_2	7.1×10^3 Ns/m	c_3	6.7×10^5 Ns/m

Table 2 Parameters for beam and foundation

Beam		Foundation	
$\overline{m}$	60 kg/m	$\overline{k}_{\mathrm{w}}$	1×10^7 N/m^2
E	2×10^{11} N/m^2	c	4900 Ns/m^2
I	3.06×10^{-5} m^4		
L	50 m		

Fig. 3 Beam displacement at the interaction point **a** Koh et al. [13], **b** Article

In the next verification, the displacement of the beam when the train moves on the beam with constant velocity, without consideration of the second foundation parameter affection (first velocity $V = 0$ m/s, then moving with constant acceleration $a_{max} = 10$ m/s^2, after 2 s it reaches the velocity $V_{max} = 20$ m/s, then it moves with constant deceleration $a_{min} = -10$ m/s^2, and it stops after 2 s. The total analyzing time is $t = 6$ s, without consideration of foundation roughness amplitude) (Fig. 4).

From these surveyed results, we compare them to those of other authors and it shows that the results from the article are well-matched with others which quote in the references. It proves the calculation program is reliability. Thence, we have the groundwork to continue to analyze the affection of foundation parameters, mass model, the roughness of the beam surface on moving beam response.
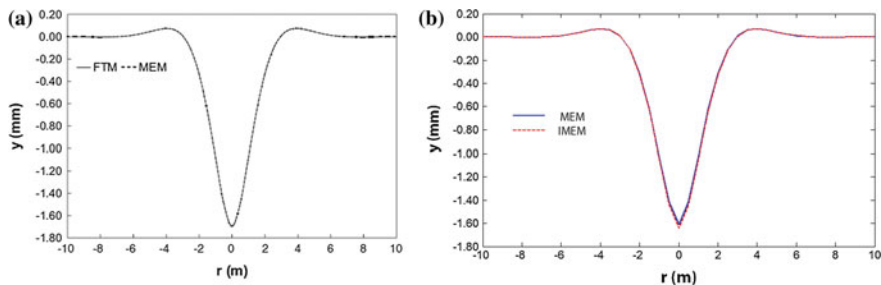
Fig. 4 Beam displacement at the interaction point **a** Koh et al. [13], **b** Article

3.2 Numerical Survey Result

The parameters of over hanging moving mass, beam and foundation of the problem which is showed in Tables 1 and 2. In case 1 and case 2, the second parameter of the foundation changes in turn to $k_s = 0$ N; 6×10^5 N; 8×10^6 N; 16×10^6 N according to Feng and Cook [20] and the load moves on the beam with constant velocity $V = 90$ m/s.

- **Case 1:** This problem keeps the roughness wavelength value $\lambda_t = 0.5$ m. Changing the roughness amplitude on beam a_t in turn to 0; 0.8; 1.6; 2.4; 3.2; and 4 mm.
- **Case 2:** This problem keeps the roughness amplitude on beam value $a_t = 1.6$ mm. Changing the roughness wavelength λ_t in turn to 0.5; 1.0; 1.5; 2.0; 2.5; 3.0; 3.5; and 4.0 m.

Figure 5 indicates the analyzed results of the dynamic response of the beam in case 1. The result shows that when increasing the second parameter of the foundation, then the value of the beam displacement also decreases; the more value of k_s increases, the more value of the beam displacement decreases. Therefore, the second parameter of the foundation is significant; it reduces dynamic response of beam system.

Also in Fig. 5, the analysis shows that when increasing the roughness amplitude on beam, the value of the beam displacement also increases. The more value of a_t increases, the more value of the beam displacement increases. This proves that the beam displacement depends on the roughness amplitude very large on beam. When the roughness amplitude on beam increases, then the beam displacement also increases likely linear with it.

Figure 6 shows the analyzed moving response in case 2. The analysis of Fig. 6 shows that the roughness wavelength on beam λ_t is small between 0.5 and 2 m; if increasing the wavelength, the beam displacement also increases. Nevertheless,

Fig. 5 Maximum displacement of the beam when keeping the value of the roughness wavelength $\lambda_t = 0.5$ m, changing the second parameter of the foundation k_s and the roughness amplitude
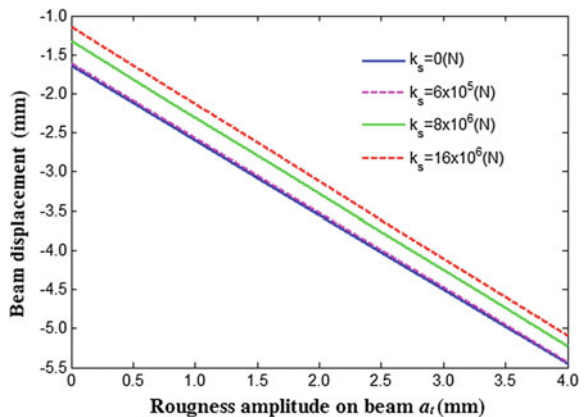
Fig. 6 Maximum beam displacement when keeping the value of the roughness amplitude on beam $a_t = 1.6$ mm, changing the second foundation parameter and the roughness wavelength
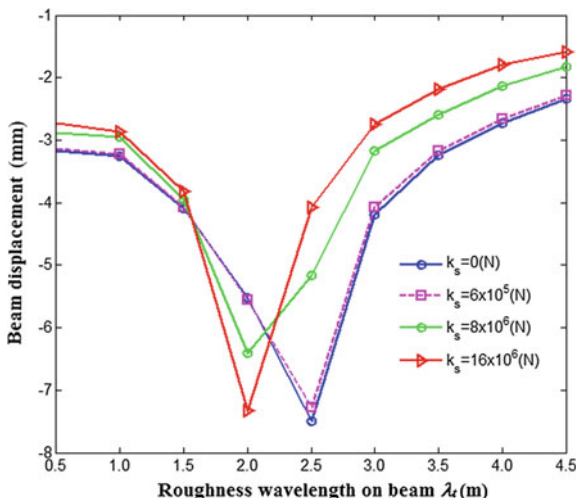
when the value of the roughness wavelength increases to a certain point, specifically in case 2, when the wavelength increases over 2.5 m then the beam displacement decreases and is asymptotic to a certain point. When the roughness wavelength on beam λ_t is between 2.0 and 2.5 m, then the beam displacement value increases and reaches the maximum point. Specifically when $k_s = 6 \times 10^6$ N, then the maximum displacement is -7.2728 mm (Table 3) with the wavelength $\lambda_t = 2.5$ m.

- **Case 3:** This problem keeps the value of the second foundation parameter $k_s = 6 \times 10^5$ (N) and the roughness amplitude on beam $a_t = 0.5$ mm. Changing the roughness wavelength λ_t in turn to 0.5; 1.0; 1.5; 2.0; 2.5; 3.0; 3.5; 4.0 m and velocity V changes in turn to 5; 10; 15; 20; 25; 30; 35; 40; 45; 50; 55; 60; 65; 70; 75; 80; 85; 90; 95; 100; 105; 110; 115; 120 (m/s).

By observing Fig. 7, we can tell that to each value of the roughness wavelength, when the velocity increases to a certain point, then the beam displacement reaches the maximum value. When the beam displacement reaches the maximum value and still velocity keeps going up, the beam displacement decreases and is asymptotic to a certain point. On the other hand, when increasing the roughness wavelength on beam, the velocity makes the displacement reach the maximum value and the beam displacement also goes up correspondently.

From the result of Table 4, we can see that to make the beam displacement reach the maximum value, then the ratio of the roughness wavelength and velocity has to be a certain value. This ratio of the roughness wavelength and velocity $T = \lambda_t/V$ is also the beam oscillation. The appearance of the maximum displacement at wavelength from 1.5 to 2.0 m is the consequence of resonance. In a way, the exciting frequency $f_c = 1/T$ will be nearly to the natural frequency $f_n = \omega/2\pi$ (Table 5).

Table 3 Maximum beam displacement when keeping the value of the roughness amplitude on beam a_t = 1.6 mm, changing the second foundation parameter and the roughness wavelength (mm)

k_s(N)	Roughness wavelength on beam λ_t (m)								
	0.5	1.0	1.5	2.0	2.5	3.0	3.5	4.0	4.5
0	−3.1675	−3.2607	−4.0924	−5.5265	−7.4960	−4.1917	−3.2315	−2.7274	−2.3422
6×10^5	−3.1407	−3.2303	−4.0812	−5.5627	−7.2728	−4.0760	−3.1701	−2.6689	−2.2891
8×10^6	−2.8864	−2.9422	−3.9535	−6.4122	−5.1626	−3.1793	−2.5893	−2.1353	−1.8190
16×10^6	−2.7215	−2.8611	−3.8147	−7.3314	−4.0752	−2.7435	−2.1871	−1.7839	−1.5846
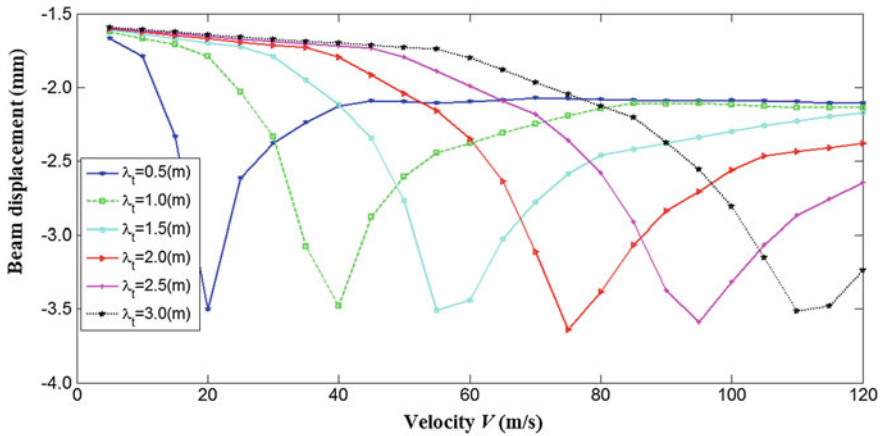
Fig. 7 Maximum beam displacement when keeping the roughness amplitude on beam $a_t = 0.5$ mm, changing velocity and the roughness wavelength

Table 4 Period and frequency of beam (mm)

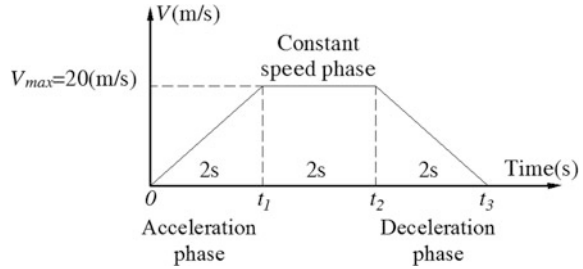| Roughness wavelength on beam λ_t (m)	Maximum displacement (mm)	Velocity V (m/s)	Period $T = \lambda/V$ (s)	Exciting frequency $f_c = 1/T$ (Hz)
0.5	−3.50179	20	0.0250	40.00
1.0	−3.47803	40	0.0250	40.00
1.5	−3.50986	55	0.0273	36.67
2.0	−3.63765	75	0.0267	37.50
2.5	−3.58805	95	0.0263	38.00
3.0	−3.51318	110	0.0273	36.67

Table 5 Natural frequency of the system in the first five modes

| Natural frequency (Hz)	Mode 1	Mode 2	Mode 3	Mode 4	Mode 5
$f_n = \omega/2\pi$	0.955	11.6	38.1	65	65

- **Case 4:** This math remains the roughness wavelength intact on beam $\lambda_t = 0.5$ m, and the second foundation parameter is 6×10^5 N. Changing the roughness amplitude on beam a_t in turn to 0; 0.8; 1.6; 2.4; 3.2; and 4 mm.
- **Case 5:** This math remains the roughness amplitude on beam $a_t = 1.6$ mm, and the second foundation parameter is 6×10^5 N. Changing of the roughness wavelength on beam λ_t in turn to 0.5; 1.0; 1.5; 2.0; 2.5; 3.0; 3.5; and 4.0 m.

In case 4 and case 5, the velocity varies as in Fig. 8. The velocity is divided into three phases (phase 1: increasing; phase 2: constant velocity; phase 3: decreasing). The original velocity of the object is $V = 0$ m/s, then it moves with constant

Fig. 8 Vehicle velocity profile

Fig. 9 Maximum beam displacement when keeping the roughness wavelength on beam λ_t = 0.5 m, changing only the roughness amplitude
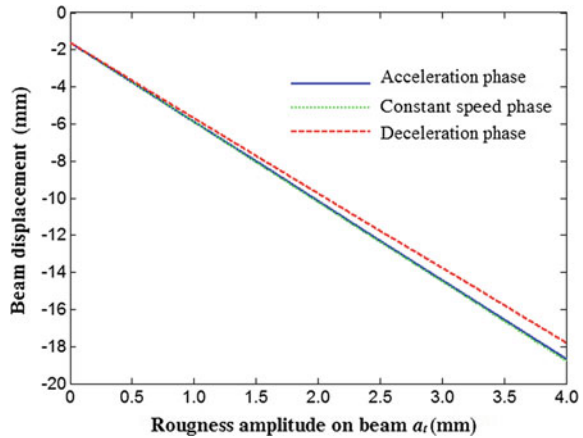

acceleration a_{max} = 10 m/s². After 2 s of acceleration, the object has the constant velocity V_{max} = 20 m/s in 2 s and moves with constant deceleration a_{min} = −10 m/s² and stops after 2 s.

Figure 9 shows the value of the beam displacement at each phase of the velocity and each value of the roughness magnitude on beam. The result shows that when increasing the roughness amplitude on beam, the value of the beam displacement increases also. Besides, other phases like acceleration, constant velocity, or deceleration do not make the value of the beam displacement increase, and these values are closely the same. Thence, the beam displacement depends very much on the roughness amplitude on beam. When the roughness amplitude increases, the value of the beam displacement also increases linearly.

Figure 10 shows the value of the beam displacement at each phase of the velocity and each value of the roughness wavelength on beam. We can tell that the bigger value of the roughness wavelength, the smaller the beam displacement of three phases of the velocity. The beam displacement decreases dramatically when the wavelength λ_t = 1.0 mm and is asymptotic to a certain point. This proves that the beam displacement is also affected by the roughness wavelength on beam.

Fig. 10 Maximum beam displacement when keeping the roughness amplitude $a_t = 1.6$ mm, changing only the roughness wavelength
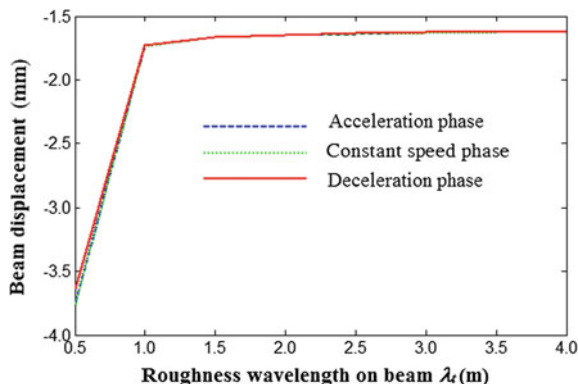
4 Conclusions

The paper presents the result on dynamic analysis of beams on two-parameter viscoelastic Pasternak foundation subjected to the moving load and considering effects of beam roughness developed with Improved Moving Element Method (IMEM). The result shows that the second foundation parameter has significant effect on dynamic response of beam; when increasing the second foundation parameter, the beam displacement also decreases. The model of two-parameter foundation has the smaller displacement than the traditional viscoelastic foundation ($k_s = 0$).

In addition, the beam roughness also has influence significantly on dynamic response of beam. When the roughness amplitude increases, the beam displacement also increases with nearly linear ratio. Besides, when the roughness wavelength is between $\lambda_t = 0.5$–2 m, the more roughness wavelength increases, the more beam displacement increases. However, when the roughness wavelength reaches to a certain point, the beam displacement will decrease and be asymptotic to a certain point.

The resonance makes the beam displacement to reach the maximum value. The cause of this resonance depends on many elements such as: the velocity of the mass, the roughness wavelength on beam, and the second foundation parameter. Therefore, it is necessary to consider the combination of all mentioned above elements in the engineering design to avoid this dangerous resonance.

When the load moves with the various accelerations, decelerations, or constant velocity, then the beam displacement depends on the roughness amplitude on beam. The beam displacement increases when the amplitude increases. Moreover, the beam displacement also varies dramatically when the roughness wavelength varies. Thus, in the engineering design, special consideration of dynamic response of moving load resting on beam with various speed is essential and correct to the real demand of the structural beam.

References

1. Winkler E (1867) Die lehre von der elastizitat und festigketit, Dominicus Prague
2. Flamenco-Borodich MM (1940) Some approximate theories of elastic foundation. Uchenyie Zapiski Moskovskogo Gosudarstvennogo Universiteta Mekhanica 46, pp 3–18 (in Russian)
3. Hetényi M (1946) Beams on elastic foundation: theory with applications in the fields of civil and mechanical engineering. University of Michigan Press, Michigan USA
4. Pasternak PL (1954) On a new method of analysis of an elastic foundation by means of two constants. Gosudarstvennoe lzdatelstvo literaturi po Stroitelstvui Arkhitekture, Moscow (in Russian)
5. Reissner E (1967) Note on the formulation of the problem of the plate on an elastic foundation. Acta Mech 4:88–91
6. Chang-Yong C, Yang Z (2008) Dynamic response of a beam on a Pasternak foundation and under a moving load. J Chongqing University (English Edition) 7(4):311–316. ISSN 1671-8224
7. Kumari S, Sahoo PP, Sawant VA (2012) Dynamic response of railway track using two parameters model. Int J Sci Eng Appl 1(2). ISSN 2319-7560
8. Luong-Van H, Nguyen-Thoi T, Liu GR, Phung-Van P (2014) A cell-based smoothed finite element method using three-node shear-locking free Mindlin plate element (CS-FEM-MIN3) for dynamic response of laminated composite plates on viscoelastic foundation. Eng Anal Boundary Elem 42:8–19
9. Phung-Van P, Nguyen-Thoi T, Luong-Van H, Thai-Hoang C, Nguyen-Xuan H (2014) A cell-based smoothed discrete shear gap method (CS-FEM-DSG3) using layerwise deformation theory for dynamic response of composite plates resting on viscoelastic foundation. Comput Methods Appl Mech Eng 272:138–159
10. Phung-Van P, Luong-Van H, Nguyen-Thoi T, Nguyen-Xuan H (2014) A cell-based smoothed discrete shear gap method (CS-FEM-DSG3) based on the C0-type higher-order shear deformation theory for dynamic responses of Mindlin plates on viscoelastic foundations subjected to a moving sprung vehicle. Int J Numer Methods Eng 98(13):988–1014
11. Nguyen-Thoi T, Luong-Van H, Phung-Van P, Rabczuk T, Tran-Trung D (2013) Dynamic responses of composite plates on the Pasternak foundation subjected to a moving mass by a cell-based smoothed discrete shear gap (CS-FEM-DSG3) method. Int J Compos Mater 3 (A):19–27
12. Lou P, Au FTK (2013) Finite element formulae for internal forces of Bernoulli-Euler beams under moving vehicles. J Sound Vib 332:1533–1552
13. Koh CG, Ong JSY, Chua DKH, Feng J (2003) Moving element for train-track dynamics. Int J Numer Methods Eng 56:1549–1567
14. Tran MT, Ang KK, Luong VH (2014) Vertical dynamic response of non-uniform motion of high-speed rails. J Sound Vib. https://dx.doi.org/10.2016/j.jsv.2014.05.053
15. Ang KK, Tran MT, Luong VH (2013) Track vibrations during accelerating and decelerating phases of high-speed rails. In: Thirteenth East Asia-Pacific conference on structural engineering and construction EASEC-13 11 Sapporo Japan
16. Ang KK, Dai J (2013) Response analysis of high-speed rail system accounting for abrupt change of foundation stiffness. J Sound Vib 332:2954–2970
17. Ang KK, Dai J, Tran MT, Luong VH (2014) Analysis of high-speed rail accounting for jumping wheel phenomenon. Int J Comput Methods 11(3):1343007-1–1343007-12. https://dx.doi.org/10.1142/S021987621343007X
18. Tran MT, Ang KK, Luong VH (2016) Vertical dynamic response of high-speed rails during sudden deceleration. Int J Comput Methods
19. Do KQ, Luong VH (2010) Structural dynamics. Ho Chi Minh City National University Publishing Company
20. Feng Z, Cook R (1983) Beam elements on two-parameter elastic foundations. J Eng Mech 109:1390–1402